

# Joint State-Parameter Observer-Based Robust Control of a UAV for Heavy Load Transportation<sup>\*</sup>

Brenner S. Rego<sup>1</sup>, Daniel N. Cardoso<sup>2</sup>, Marco. H. Terra<sup>1</sup>, and Guilherme V. Raffo<sup>2</sup>

<sup>1</sup> University of São Paulo, São Carlos, SP 13566-590, Brazil,  
brennersr7@usp.br, terra@sc.usp.br,

<sup>2</sup> Federal University of Minas Gerais, Belo Horizonte, MG 31270-901, Brazil,  
{danielneri, raffo}@ufmg.br

**Abstract** This paper proposes a joint state-parameter observer-based controller for trajectory tracking of an octocopter unmanned aerial vehicle (OUAV), for transportation of a heavy load with unknown mass and size. The multi-body dynamic model of the OUAV with a rigidly attached load is obtained, effectively considering the effects of the load parameters into the dynamics of the system. A robust nonlinear  $\mathcal{W}_\infty$  control strategy is designed for optimal trajectory tracking of the OUAV, with information of the states and load parameters provided by a joint estimation unscented Kalman filter. The effectiveness of the proposed strategy is corroborated by numerical results.

**Keywords:** Aerial load transportation, Nonlinear Robust Control, State and Parameter Estimation.

## 1 Introduction

Taking advantage of their versatility and autonomous operation, unmanned aerial vehicles (UAVs) can be used for aerial load transportation, with many applications such as vertical replenishment of seaborne vessels [11], deployment of supplies in search-and-rescue missions [1], package delivery, and landmine detection [2]. Aerial load transportation using UAVs is a challenging task in terms of modeling and control. The load may be connected to the UAV either rigidly or by means of a rope, which changes its dynamics considerably. In addition, the load physical parameters are often unknown in practice, and their knowledge is usually necessary to effectively accomplish the task. A model-free control approach based on trajectory generation by reinforcement learning has been proposed in [7] for path tracking of the load using a quadrotor UAV (QUAV).

---

<sup>\*</sup> This work was in part supported by the project INCT (National Institute of Science and Technology) for Cooperative Autonomous Systems Applied to Security and Environment under the grants CNPq 465755/2014-3 and FAPESP 2014/50851-0, and by the Brazilian agencies CAPES under the grant numbers 88887.136349/2017-00 and 001, CNPq under the grant 315695/2020-0, FAPEMIG under the grant APQ-03090-17, and FAPESP under the grant 2022/05052-8.

However, this is an open-loop method, and the entire learning process must be repeated if there are any changes in the system. A hybrid control strategy has been proposed in [10] addressing a similar transportation problem, relying on a decoupling-based cascade structure, and considering the case in which the cable is taut and when it is loose. However, the strategy is not robust to external disturbances and unmodeled dynamics.

Although several works have investigated the load transportation problem, only a few propose estimation techniques to obtain information on the load physical parameters, which are important to achieve effectiveness in the task. An unscented Kalman filter (UKF) has been designed in [3] to estimate the load's position and velocity for a helicopter with suspended load. The authors have also proposed methods for estimating the wire's length. This algorithm has been combined with delayed adaptive feedback control, taking advantage of the wire's length estimation. Nevertheless, other physical parameters such as the load mass, are assumed to be known. State and parameter estimation has been addressed in [8] for load transportation using a QUAV. The proposed methodology estimates the angles and length of the cable; however, it assumes the load mass to be precisely known, in addition to disregard the load inertia tensor, being unsuitable for heavy load transportation. Adaptive control has been investigated in [12] considering the estimation of the load mass, but the rotational dynamics of the load have been once again neglected. Lastly, a geometric control strategy based on an inner-outer loop structure with disturbance estimation has been proposed in [5]. Nevertheless, it has used a simplified model where the inertia tensor of the load has been again neglected.

In view of these challenges, we propose a joint state-parameter observer-based controller for trajectory tracking of an octocopter UAV (OUAV) that carries a heavy load of unknown mass and size. The contributions are threefold: (i) the multi-body dynamic modeling of the OUAV with a rigidly attached heavy load; (ii) the design of a novel robust nonlinear control strategy with fast disturbances attenuation for load transportation of the OUAV, based on the proposal of a new particular solution to the nonlinear  $\mathcal{W}_\infty$  control problem [4]; and (iii) the design of a UKF-based algorithm for robust joint estimation of the OUAV states, exogenous disturbances, and the load parameters, which are provided to the nonlinear  $\mathcal{W}_\infty$  controller for efficient trajectory tracking of the OUAV with load.

## 2 Octocopter UAV Modeling

In this work, the UAV equations of motion are obtained using the Euler-Lagrange formalism (ELF) [9], considering the UAV and the load as two rigidly attached bodies. We define four reference frames (see Figure 1): the inertial frame  $\mathcal{I}$ , the body frame  $\mathcal{B}$ , which is rigidly attached to the OUAV, and the frames  $\mathcal{C}_O$  and  $\mathcal{C}_L$  that are rigidly attached at the centers of mass (COMs) of the OUAV and load, respectively.

The OUAV is assumed to have six degrees of freedom (DOF), being the generalized coordinates vector defined as  $\mathbf{q}(t) \triangleq [\boldsymbol{\xi}' \boldsymbol{\eta}']'$ , where  $\boldsymbol{\eta}(t) \triangleq [\phi \ \theta \ \psi]'$ ,

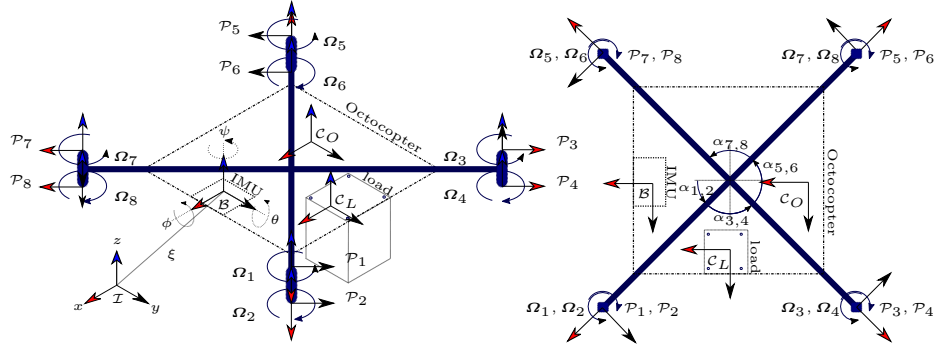


**Figure 1.** Definitions: propeller velocities  $\Omega_p$  and frames  $\mathcal{P}_p$ , COMs frames  $\mathcal{C}_O$ ,  $\mathcal{C}_L$ , inertial frame  $\mathcal{I}$ , body frame  $\mathcal{B}$ , and angles  $\alpha_p$ , with  $p \in \{1, \dots, 8\}$ .

is the orientation of  $\mathcal{B}$  w.r.t.  $\mathcal{I}$  described by the Euler angles using the ZYX convention about the local axes, with  $\phi(t), \theta(t), \psi(t) \in \mathbb{R}$ ; and  $\xi(t) \triangleq [x \ y \ z]'$  is the position of the origin of frame  $\mathcal{B}$  w.r.t.  $\mathcal{I}$ , with  $x(t), y(t), z(t) \in \mathbb{R}$ . Accordingly, the orientation and position of the origin of  $\mathcal{B}$  w.r.t.  $\mathcal{I}$  are given, respectively, by<sup>3</sup>  $\mathbf{R}_{\mathcal{B}}^{\mathcal{I}} = \mathbf{R}_{z,\psi} \mathbf{R}_{y,\theta} \mathbf{R}_{x,\phi}$ , and  $\mathbf{p}_{\mathcal{I},\mathcal{B}}^{\mathcal{I}} = \xi$ , and the orientation and position of the COMs of the OUAV and load are  $\mathbf{R}_i^{\mathcal{I}} = \mathbf{R}_{\mathcal{B}}^{\mathcal{I}}$ , and  $\mathbf{p}_{\mathcal{I},i}^{\mathcal{I}} = \mathbf{p}_{\mathcal{I},\mathcal{B}}^{\mathcal{I}} + \mathbf{R}_{\mathcal{B}}^{\mathcal{I}} \mathbf{d}_{\mathcal{B},i}^{\mathcal{B}}$ , for  $i \in \{\mathcal{C}_O, \mathcal{C}_L\}$ , where  $\mathbf{d}_{\mathcal{B},i}^{\mathcal{B}} \in \mathbb{R}^3$  is the position of the origin of frame  $i$  w.r.t.  $\mathcal{B}$ .

The linear velocities of the COMs of the OUAV and load are computed through the time derivative of their respective positions

$$\dot{\mathbf{p}}_{\mathcal{I},i}^{\mathcal{I}} = \mathbf{v}_{\mathcal{I},i}^{\mathcal{I}} = \dot{\xi} + \mathbf{R}_{\mathcal{B}}^{\mathcal{I}} \mathbf{S}(\mathbf{w}_{\mathcal{I},\mathcal{B}}^{\mathcal{B}}) \mathbf{d}_{\mathcal{B},i}^{\mathcal{B}} = [\mathbf{I} - \mathbf{R}_{\mathcal{B}}^{\mathcal{I}} \mathbf{S}(\mathbf{d}_{\mathcal{B},i}^{\mathcal{B}}) \mathbf{W}_{\eta}] \dot{\mathbf{q}} = \mathbf{J}_i \dot{\mathbf{q}}, \quad (1)$$

where  $\mathbf{J}_i$  is the linear velocity Jacobian,  $\mathbf{w}_{\mathcal{I},\mathcal{B}}^{\mathcal{B}} \triangleq \mathbf{W}_{\eta} \dot{\boldsymbol{\eta}}$  is the OUAV angular velocity vector, with  $\mathbf{w}_{\mathcal{I},\mathcal{B}}^{\mathcal{B}} \in \mathbb{R}^3$ , and  $\mathbf{W}_{\eta} \triangleq \begin{bmatrix} 1 & 0 & -\sin(\theta) \\ 0 & \cos(\phi) & \cos(\theta) \sin(\phi) \\ 0 & -\sin(\phi) & \cos(\phi) \cos(\theta) \end{bmatrix}$  is the Euler

matrix. Besides, we used the properties  $\mathbf{R}_{\mathcal{B}}^{\mathcal{I}} = \mathbf{R}_{\mathcal{B}}^{\mathcal{I}} \mathbf{S}(\mathbf{w}_{\mathcal{I},\mathcal{B}}^{\mathcal{B}})$  and  $\mathbf{S}(\mathbf{w}_{\mathcal{I},\mathcal{B}}^{\mathcal{B}}) \mathbf{d}_{\mathcal{B},i}^{\mathcal{B}} = -\mathbf{S}(\mathbf{d}_{\mathcal{B},i}^{\mathcal{B}}) \mathbf{w}_{\mathcal{I},\mathcal{B}}^{\mathcal{B}}$ , where  $\mathbf{S}(\cdot) \in \mathbb{R}^{3 \times 3}$  is a skew-symmetric matrix [9]. In addition, the angular velocities of the COMs of the OUAV and load are given by

$$\mathbf{w}_{\mathcal{I},i}^{\mathcal{I}} = \mathbf{R}_{\mathcal{B}}^{\mathcal{I}} \mathbf{w}_{\mathcal{I},\mathcal{B}}^{\mathcal{B}} = \mathbf{R}_{\mathcal{B}}^{\mathcal{I}} \mathbf{W}_{\eta} \dot{\boldsymbol{\eta}} = [\mathbf{0} \ \mathbf{R}_{\mathcal{B}}^{\mathcal{I}} \mathbf{W}_{\eta}] \dot{\mathbf{q}} = \mathbf{W}_i \dot{\mathbf{q}}, \quad \mathbf{W}_i \triangleq [\mathbf{0} \ \mathbf{R}_{\mathcal{B}}^{\mathcal{I}} \mathbf{W}_{\eta}]. \quad (2)$$

Using the ELF [9], the OUAV equations of motion are written as

$$\mathbf{M}(\mathbf{q}) \ddot{\mathbf{q}}(t) + \mathbf{C}(\mathbf{q}, \dot{\mathbf{q}}) \dot{\mathbf{q}}(t) + \mathbf{g}(\mathbf{q}) = \boldsymbol{\vartheta}(\mathbf{q}, \boldsymbol{\tau}) + \boldsymbol{\zeta}(t), \quad (3)$$

where  $\mathbf{M}(\mathbf{q}) \in \mathbb{R}^{6 \times 6}$  is the inertia matrix,  $\mathbf{C}(\mathbf{q}, \dot{\mathbf{q}}) \in \mathbb{R}^{6 \times 6}$  is the Coriolis and centripetal forces matrix,  $\mathbf{g}(\mathbf{q}) \in \mathbb{R}^6$  is the gravitational force vector,  $\boldsymbol{\vartheta}(\mathbf{q}, \boldsymbol{\tau}) \in$

<sup>3</sup> Throughout the manuscript, some function dependencies are omitted. Moreover,  $\mathbf{I}$  and  $\mathbf{0}$  are identity and zero matrices, respectively, with appropriate dimensions;  $\|\mathbf{z}(t)\|_{\mathcal{W}_{\kappa,p,\Gamma}} \triangleq (\sum_{\alpha=0}^{\kappa} \|d^{\alpha} \mathbf{z}(t)/dt^{\alpha}\|_{\mathcal{L}_p, \Gamma_{\alpha}}^p)^{1/p}$ , with  $\Gamma \triangleq \{\Gamma_0, \dots, \Gamma_{\kappa}\}$ , where  $p \in \mathbb{N} \cup \{\infty\}$ ,  $\kappa \in \mathbb{N} \cup \{0\}$  and  $\|\mathbf{z}(t)\|_{\mathcal{L}_p, \Gamma_{\alpha}} \triangleq (\int_0^{\infty} \|\Gamma_{\alpha}^{1/p} \mathbf{z}(t)\|_p^p dt)^{\frac{1}{p}}$ , in which  $\Gamma_{\alpha} > 0$ ; and  $\partial_t V \triangleq \partial V / \partial t$ ,  $\partial_{\chi} V \triangleq \partial V / \partial \chi$ .

$\mathbb{R}^6$  is the vector of generalized inputs, with  $\boldsymbol{\tau}(t) \triangleq [f_{\mathcal{P}_1} f_{\mathcal{P}_2} \cdots f_{\mathcal{P}_8}]'$ , in which  $f_p(t)$  is the force applied by the  $p$ -th propeller, for  $p \in \{1, 2, \dots, 8\}$ , and  $\boldsymbol{\zeta}(t) \triangleq [\zeta_x \zeta_y \zeta_z \zeta_\phi \zeta_\theta \zeta_\psi]'$ , with  $\boldsymbol{\zeta}(t) \in \mathbb{R}^6$ , is the vector of generalized disturbances.

Taking into account (1) and (2), the inertia matrix is obtained from the system total kinetic energy  $\mathcal{K}(\mathbf{q}, \dot{\mathbf{q}}) = \sum_{i \in \{C_O, C_L\}} \frac{1}{2} (m_i (\mathbf{v}_{\mathcal{I},i}^{\mathcal{I}})' \mathbf{v}_{\mathcal{I},i}^{\mathcal{I}} + (\mathbf{w}_{\mathcal{I},i}^{\mathcal{I}})' \mathbf{R}_i^{\mathcal{I}} \mathbf{I}_i \mathbf{R}_i^{\mathcal{I}'} \mathbf{w}_{\mathcal{I},i}^{\mathcal{I}}) \triangleq \frac{1}{2} \dot{\mathbf{q}}' \mathbf{M}(\mathbf{q}) \dot{\mathbf{q}} = \frac{1}{2} \dot{\mathbf{q}}' \begin{bmatrix} \mathbf{M}_{11} & \mathbf{M}_{21}' \\ \mathbf{M}_{21} & \mathbf{M}_{22} \end{bmatrix} \dot{\mathbf{q}}$ , where  $\mathbf{M}_{11} \triangleq (m_{C_O} + m_{C_L}) \mathbf{I}$ ,  $\mathbf{M}_{22} \triangleq \mathbf{W}_\eta' (-m_{C_O} \mathbf{S}(\mathbf{d}_{B,C_O}^B)^2 - m_{C_L} \mathbf{S}(\mathbf{d}_{B,C_L}^B)^2) \mathbf{W}_\eta + \mathbf{W}_\eta' (\mathbb{I}_{C_O} + \mathbb{I}_{C_L}) \mathbf{W}_\eta$ ,  $\mathbf{M}_{12} \triangleq -\mathbf{R}_B^{\mathcal{I}} (m_{C_O} \mathbf{S}(\mathbf{d}_{B,C_O}^B) + m_{C_L} \mathbf{S}(\mathbf{d}_{B,C_L}^B)) \mathbf{W}_\eta$ , and  $m_i \in \mathbb{R}$  and  $\mathbb{I}_i \in \mathbb{R}^{3 \times 3}$  are, respectively, the mass and the inertia tensor matrix of the body whose  $i$ -th frame is rigidly attached. The gravitational force vector is given by  $\mathbf{g}(\mathbf{q}) = \partial_{\mathbf{q}} \mathcal{P}(\mathbf{q})$ , where  $\mathcal{P}(\mathbf{q}) = -\sum_{i \in \{C_O, C_L\}} m_i \mathbf{g}_r \mathbf{p}_{\mathcal{I},i}^{\mathcal{I}}$  is the system total potential energy, and  $\mathbf{g}_r \triangleq [0 \ 0 \ g]'$ , in which  $g$  is the gravitational acceleration, while  $\mathbf{C}(\mathbf{q}, \dot{\mathbf{q}})$  is obtained from  $\mathbf{M}(\mathbf{q})$  by computing the Christoffel symbols of first kind [9].

The force and torque generated by the  $p$ -th propeller,  $p \in \{1, 2, \dots, 8\}$ , are assumed to be applied at its geometric center. Then, to compute  $\boldsymbol{\vartheta}(\mathbf{q}, \boldsymbol{\tau})$ , a frame is rigidly attached to the geometric center of the  $p$ -th propeller, denoted by  $\mathcal{P}_p$ , as illustrated in Figure 1. Accordingly, the orientation and position of the origin of  $\mathcal{P}_p$  w.r.t.  $\mathcal{I}$  are, respectively,  $\mathbf{R}_{\mathcal{P}_p}^{\mathcal{I}} = \mathbf{R}_B^{\mathcal{I}}$ , and  $\mathbf{p}_{\mathcal{I},\mathcal{P}_p}^{\mathcal{I}} = \boldsymbol{\xi} + \mathbf{R}_B^{\mathcal{I}} \mathbf{d}_{B,\mathcal{P}_p}^B$ , from which

$$\mathbf{w}_{\mathcal{I},\mathcal{P}_p}^{\mathcal{I}} = \mathbf{w}_{\mathcal{I},B}^{\mathcal{I}} = \mathbf{R}_B^{\mathcal{I}} \mathbf{w}_{\mathcal{I},B}^B = [\mathbf{0} \ \mathbf{R}_B^{\mathcal{I}} \mathbf{W}_\eta] \dot{\mathbf{q}} \triangleq \mathbf{W}_{\mathcal{P}_p} \dot{\mathbf{q}}, \quad (4)$$

$$\dot{\mathbf{p}}_{\mathcal{I},\mathcal{P}_p}^{\mathcal{I}} = \mathbf{v}_{\mathcal{I},\mathcal{P}_p}^{\mathcal{I}} = \dot{\boldsymbol{\xi}} - \mathbf{R}_B^{\mathcal{I}} \mathbf{S}(\mathbf{d}_{B,\mathcal{P}_p}^B) \mathbf{W}_\eta \dot{\boldsymbol{\eta}} = [\mathbf{I} - \mathbf{R}_B^{\mathcal{I}} \mathbf{S}(\mathbf{d}_{B,\mathcal{P}_p}^B) \mathbf{W}_\eta] \dot{\mathbf{q}} \triangleq \mathbf{J}_{\mathcal{P}_p} \dot{\mathbf{q}}. \quad (5)$$

The thrust and torque generated by each propeller are given, respectively, by

$$f_{\mathcal{P}_p}(t) = b \boldsymbol{\Omega}_p^2(t), \quad \tau_{\mathcal{P}_p}(t) = \lambda_{\mathcal{P}_p} k_\tau \boldsymbol{\Omega}_p^2(t), \quad (6)$$

where  $k_\tau \in \mathbb{R}$  and  $b \in \mathbb{R}$  are the propeller's drag and thrust constants,  $\boldsymbol{\Omega}_p(t) \in \mathbb{R}$  is propeller's angular velocity, and  $\lambda_{\mathcal{P}_p} \in \{1, -1\}$  relates to the direction of rotation of the  $p$ -th propeller, in top view: if clockwise,  $-1$ , if counter-clockwise,  $1$ .

Taking into account (6), (5) and (4), the contribution of the  $p$ -th propeller to the vector of generalized coordinates is given by  $\boldsymbol{\vartheta}_{\mathcal{P}_p} = \mathbf{J}_{\mathcal{P}_p}' \mathbf{R}_{\mathcal{P}_p}^{\mathcal{I}} \mathbf{a}_z f_{\mathcal{P}_p}(t) + \mathbf{W}_{\mathcal{P}_p}' \mathbf{R}_{\mathcal{P}_p}^{\mathcal{I}} \mathbf{a}_z \tau_{\mathcal{P}_p}(t) = (\mathbf{J}_{\mathcal{P}_p}' + \mathbf{W}_{\mathcal{P}_p}' \lambda_{\mathcal{P}_p} k_b) \mathbf{R}_{\mathcal{P}_p}^{\mathcal{I}} \mathbf{a}_z f_{\mathcal{P}_p}(t)$ , where  $\mathbf{a}_z \triangleq [0 \ 0 \ 1]'$ , and  $k_b \triangleq k_\tau/b$ . Therefore, the vector of generalized input is  $\boldsymbol{\vartheta}(\mathbf{q}, \mathbf{u}) = \sum_{p=1}^8 \boldsymbol{\vartheta}_{\mathcal{P}_p}$ , yielding

$$\boldsymbol{\vartheta}(\mathbf{q}, \mathbf{u}) = \mathbf{B}(\mathbf{q}) \boldsymbol{\tau} \triangleq [\boldsymbol{\Xi}_1 \mathbf{a}_z \cdots \boldsymbol{\Xi}_8 \mathbf{a}_z] \boldsymbol{\tau}, \quad \boldsymbol{\Xi}_i \triangleq (\mathbf{J}_{\mathcal{P}_i}' + \mathbf{W}_{\mathcal{P}_i}' \lambda_{\mathcal{P}_i} k_b) \mathbf{R}_{\mathcal{P}_i}^{\mathcal{I}}. \quad (7)$$

### 3 Nonlinear $\mathcal{W}_\infty$ control of the Octocopter UAV

Before designing the nonlinear controller for the OUAV, the  $\mathcal{W}_\infty$  control problem is stated considering a general second-order nonlinear nonautonomous dynamical system, and a particular solution to the resulting Hamilton-Jacobi (HJ) equation is proposed. Unlike in [4], this solution requires solving a single Riccati equation.

**Theorem 1.** *Consider the nonlinear system*

$$\dot{\boldsymbol{\chi}}(t) = \mathbf{f}(\boldsymbol{\chi}, t) + \mathbf{G}(\boldsymbol{\chi}, t) \mathbf{u}(t) + \mathbf{K}(\boldsymbol{\chi}, t) \mathbf{w}(t), \quad \mathbf{z}(t) = \int_0^t \tilde{\mathbf{q}}(\tau) d\tau, \quad (8)$$

with  $\mathbf{f}(\boldsymbol{\chi}, t) \triangleq [\dot{\mathbf{q}}'(t) \dot{\mathbf{q}}'(t) \mathbf{h}'(\boldsymbol{\chi}, t)]'$ ,  $\mathbf{G}(\boldsymbol{\chi}, t) = \mathbf{K}(\boldsymbol{\chi}, t) = [\mathbf{0} \ \mathbf{0} \ (\mathbf{M}^{-1}(\boldsymbol{\chi}, t))']'$ , where  $\mathbf{u} \in \mathbb{R}^{n_u}$  is the input vector,  $\mathbf{w} \in \mathbb{R}^{n_w}$  is the disturbance vector,  $\tilde{\mathbf{q}} \triangleq \mathbf{q} - \mathbf{q}_r$ , where  $\mathbf{q}(t) \in \mathbb{R}^{n_q}$  are the generalized coordinates,  $\mathbf{q}_r \in \mathcal{C}^2$  is the desired reference, and  $\boldsymbol{\chi} \triangleq [\int_0^t \dot{\mathbf{q}}'(\tau) d\tau \ \tilde{\mathbf{q}}'(t) \ \dot{\mathbf{q}}'(t)]'$  is the state vector. Let  $\text{rank}(\mathbf{M}(\boldsymbol{\chi}, t)) = n_q$ , for any  $\boldsymbol{\chi} \in \Omega$  and  $t \in \mathbb{R}_{\geq 0}$ , where  $\Omega$  stands for the set of all configurations the system can assume, with  $n_q = n_u$ . Therefore, a control law that satisfies the nonlinear  $\mathcal{W}_\infty$  optimal control (OC) problem

$$\min_{\mathbf{u} \in \mathcal{U}} \max_{\mathbf{w} \in \mathcal{D}} 0.5 \|\mathbf{z}(t)\|_{\mathcal{W}_{3,2,\mathbf{Y}}}^2 - 0.5\gamma^2 \|\mathbf{w}(t)\|_{\mathcal{L}_2}^2, \quad \text{s.t.} \quad (8), \quad (9)$$

for a given sufficiently large  $\mathcal{W}_\infty$ -index  $\gamma \in \mathbb{R}_{\geq 0}$  and weighting matrices  $\mathbf{Y} = (\mathbf{Y}_0, \mathbf{Y}_1, \mathbf{Y}_2, \mathbf{Y}_3)$ , such that  $\mathcal{U} = \mathbb{R}^{n_u}$  and  $\mathcal{D} = \mathcal{L}_2[0, \infty)$ , is given by

$$\mathbf{u}(t) = -\mathbf{M}([\mathbf{0} \ \mathbf{0} \ (\mathbf{Y}_3)^{-1}] \mathbf{Q}\boldsymbol{\chi} + \mathbf{h}(\boldsymbol{\chi}, t)), \quad \text{s.t.} \quad \mathbf{Q}\mathbf{A} + \mathbf{A}'\mathbf{Q} - \mathbf{Q}\mathbf{B}\mathbf{Q} + \boldsymbol{\Psi} = \mathbf{0}, \quad (10)$$

with  $\mathbf{Q} > 0$ ,  $\mathbf{A} \triangleq \begin{bmatrix} \mathbf{0} & \mathbf{I} \\ \mathbf{0} & \mathbf{0} \end{bmatrix}$ ,  $\mathbf{B} \triangleq \text{blkdiag}(\mathbf{0}, \mathbf{0}, (\mathbf{Y}_3)^{-1})$ , and  $\boldsymbol{\Psi} \triangleq \text{blkdiag}(\mathbf{Y}_0, \mathbf{Y}_1, \mathbf{Y}_2)$ .

*Proof.* By formulating the OC problem (9) via dynamic programming, using differential game theory, the associated HJBI (Hamilton-Jacobi-Bellman-Isaacs) equation is given by

$$\partial_t V_\infty + \min_{\tau \in \mathcal{U}} \max_{\mathbf{w} \in \mathcal{D}} \{\mathbb{H}_\infty(V_\infty, \boldsymbol{\chi}, \mathbf{u}, \mathbf{w}, t)\} = 0, \quad (11)$$

with the Hamiltonian  $\mathbb{H}_\infty \triangleq \partial_{\boldsymbol{\chi}}' V_\infty \dot{\boldsymbol{\chi}} + 0.5(\mathbf{z}' \mathbf{Y}_0 \mathbf{z} + \dot{\mathbf{z}}' \mathbf{Y}_1 \dot{\mathbf{z}} + \ddot{\mathbf{z}}' \mathbf{Y}_2 \ddot{\mathbf{z}} + \ddot{\mathbf{z}}' \mathbf{Y}_3 \ddot{\mathbf{z}} - \gamma^2 \mathbf{w}' \mathbf{w})$ , and boundary condition  $V_\infty(\mathbf{0}, t) = 0$ . Considering  $\boldsymbol{\Psi}$  as in the statement of the theorem, the Hamiltonian  $\mathbb{H}_\infty$  is written in its expanded form as

$$\begin{aligned} \mathbb{H}_\infty = & \partial_{\boldsymbol{\chi}}' V_\infty (\mathbf{f}(\boldsymbol{\chi}, t) + \mathbf{G}(\boldsymbol{\chi}, t) \mathbf{u} + \mathbf{K}(\boldsymbol{\chi}, t) \mathbf{w}) + 0.5 \boldsymbol{\chi}' \boldsymbol{\Psi} \boldsymbol{\chi} \\ & + 0.5 [\mathbf{h}' \mathbf{Y}_3 \mathbf{h} + \mathbf{u}' (\mathbf{M}^{-1})' \mathbf{Y}_3 \mathbf{M}^{-1} \mathbf{u} + \mathbf{w}' (\mathbf{M}^{-1})' \mathbf{Y}_3 \mathbf{M}^{-1} \mathbf{w} + 2 \mathbf{h}' \mathbf{Y}_3 \mathbf{M}^{-1} \mathbf{u} \\ & + 2 \mathbf{h}' \mathbf{Y}_3 \mathbf{M}^{-1} \mathbf{w} + 2 \mathbf{u}' (\mathbf{M}^{-1})' \mathbf{Y}_3 \mathbf{M}^{-1} \mathbf{w}] - 0.5 \gamma^2 \mathbf{w}' \mathbf{w}. \end{aligned} \quad (12)$$

The OC law,  $\mathbf{u}^*$ , and the worst case of the disturbances,  $\mathbf{w}^*$ , are obtained through the partial derivatives of (12), as follows:

$$\partial_{\mathbf{u}} \mathbb{H}_\infty = \mathbf{G}' \partial_{\boldsymbol{\chi}} V_\infty + (\mathbf{M}^{-1})' \mathbf{Y}_3 (\mathbf{M}^{-1} \mathbf{u}^* + \mathbf{h} + \mathbf{M}^{-1} \mathbf{w}^*) = 0, \quad (13)$$

$$\partial_{\mathbf{w}} \mathbb{H}_\infty = \mathbf{K}' \partial_{\boldsymbol{\chi}} V_\infty + (\mathbf{M}^{-1})' \mathbf{Y}_3 (\mathbf{M}^{-1} \mathbf{w}^* + \mathbf{h} + \mathbf{M}^{-1} \mathbf{u}^*) - \gamma^2 \mathbf{w}^* = 0. \quad (14)$$

Thus, considering (13), the OC law is given by

$$\begin{aligned} \mathbf{u}^* = & -((\mathbf{M}^{-1})' \mathbf{Y}_3 \mathbf{M}^{-1})^{-1} (\mathbf{G}' \partial_{\boldsymbol{\chi}} V_\infty + (\mathbf{M}^{-1})' \mathbf{Y}_3 (\mathbf{h} + \mathbf{M}^{-1} \mathbf{w}^*)), \\ = & -\mathbf{M}([\mathbf{0} \ \mathbf{0} \ (\mathbf{Y}_3)^{-1}] \partial_{\boldsymbol{\chi}} V_\infty + \mathbf{h}(\boldsymbol{\chi}, t) + \mathbf{w}^*). \end{aligned} \quad (15)$$

The worst case of the disturbances,  $\mathbf{w}^*$ , is computed by subtracting (14) from (13), which yields

$$\mathbf{w}^* = (1/\gamma^2) (\mathbf{K} - \mathbf{G})' \partial_{\boldsymbol{\chi}} V_\infty. \quad (16)$$

Through the second order partial derivatives of (13) and (14), which are given, respectively, by  $\partial_{\mathbf{u}}^2 \mathbb{H}_\infty = (\mathbf{M}^{-1})' \mathbf{Y}_3 \mathbf{M}^{-1} > 0$ , and  $\partial_{\mathbf{w}}^2 \mathbb{H}_\infty = (\mathbf{M}^{-1})' \mathbf{Y}_3 \mathbf{M}^{-1} - \gamma^2 \mathbf{I} <$

0, it can be verified that (15) and (16) are a Min-Max extremum of the OC problem for a sufficiently large  $\gamma$ .

The HJ PDE associated to the problem is obtained by replacing the OC law (15), and the worst case of the disturbances (16), in (11), yielding

$$\partial_t V_\infty(\chi, t) + \mathbb{H}_\infty(V_\infty, \chi, \mathbf{u}^*, \mathbf{w}^*, t) = 0. \quad (17)$$

Therefore, assuming  $V_\infty(\chi) = 0.5\chi'Q\chi > 0$ , we have that  $\partial_t V_\infty = 0$ . Consequently, (17) becomes

$$\mathbb{H}_\infty(V_\infty, \chi, \mathbf{u}^*, \mathbf{w}^*, t) = \partial'_\chi V_\infty \dot{\chi} + 0.5\chi' \Psi \chi + 0.5\ddot{\mathbf{q}}'(\mathcal{Y}_3)^{-1}\ddot{\mathbf{q}} = 0. \quad (18)$$

Taking into account (8) and (16), we have that  $\mathbf{w}^* = \mathbf{0}$ , and from (15), we have that  $\mathbf{u}^* = -\mathbf{M}([\mathbf{0} \ \mathbf{0} \ (\mathcal{Y}_3)^{-1}] Q\chi + \mathbf{h}(\chi, t))$ , which leads to  $\ddot{\mathbf{q}} = [\mathbf{0} \ \mathbf{0} - (\mathcal{Y}_3)^{-1}] Q\chi$ , and the closed-loop (CL) state-space dynamics  $\dot{\chi} = [\dot{\mathbf{q}}' \ \dot{\mathbf{q}}' \ \ddot{\mathbf{q}}']' = \mathbf{A}\chi + \mathbf{B}Q\chi$ , with  $\mathbf{A}$  and  $\mathbf{B}$  defined as in the statement of the theorem. By replacing these expressions for  $\ddot{\mathbf{q}}$  and  $\dot{\chi}$  in (18), we obtain the Riccati equation  $QA + A'Q - QBQ + \Psi = 0$ , which concludes the proof.  $\square$

**Theorem 2.** Let  $\mathbf{q}_r \in \mathcal{C}^2$  and  $\text{rank}(\mathbf{M}(\chi, t)) = n_q$ , for any  $\chi \in \Omega$  and  $t \in \mathbb{R}_{\geq 0}$ . Therefore, the control law (10) provides asymptotic stability to system (8).

*Proof.* Let  $\tilde{\chi} \triangleq (\chi, \ddot{\mathbf{q}})$ . As previously demonstrated, the CL system (8) with the control law (10) ensures (18) holds. Consequently, we have that  $\partial'_\chi V_\infty \dot{\chi} = -0.5\tilde{\chi}'\Theta\tilde{\chi}$ , with  $\Theta \triangleq \text{blkdiag}(\Psi, \mathcal{Y}_3) > 0$ , which means that  $V_\infty(\chi) > 0$  is a Lyapunov function that ensures asymptotic stability to the CL system.  $\square$

To design the nonlinear  $\mathcal{W}_\infty$  controller for the OUAV, system (3) is partitioned into controlled,  $\mathbf{q}_c$ , and regulated DOF,  $\mathbf{q}_r$ ,

$$\begin{bmatrix} M_{cc} & M_{cr} \\ M_{rc} & M_{rr} \end{bmatrix} \ddot{\mathbf{q}}(t) + \begin{bmatrix} C_{cc} & C_{cr} \\ C_{rc} & C_{rr} \end{bmatrix} \dot{\mathbf{q}}(t) + \begin{bmatrix} \mathbf{g}_c \\ \mathbf{g}_r \end{bmatrix} = \begin{bmatrix} \mathbf{B}_c \\ \mathbf{B}_r \end{bmatrix} \boldsymbol{\tau} + \mathbf{w}(t), \quad (19)$$

where  $\mathbf{q}(t) \in \mathbb{R}^6$ , with  $\mathbf{q}(t) = [\mathbf{q}'_c(t) \ \mathbf{q}'_r(t)]'$ , in which  $\mathbf{q}_c(t) \triangleq [x(t) \ y(t) \ z(t)]'$  corresponds to the controlled DOF and  $\mathbf{q}_r(t) \triangleq [\phi(t) \ \theta(t) \ \psi(t)]'$  to the regulated DOF, and  $\mathbf{w}(t) = [\mathbf{w}'_c \ \mathbf{w}'_r]'$ . Then, from (19) and considering  $\tilde{\mathbf{q}}_c = \mathbf{q}_c - \mathbf{q}_{c_r}$ , we take into account the tracking error dynamics of the controlled DOF,

$$\ddot{\tilde{\mathbf{q}}}_c = M_{cc}^{-1}(-M_{cr}\ddot{\mathbf{q}}_r - C_{cc}\dot{\tilde{\mathbf{q}}}_c - C_{cr}\dot{\mathbf{q}}_r - \mathbf{g}_c) + M_{cc}^{-1}\mathbf{u} + M_{cc}^{-1}\mathbf{w}_c - \ddot{\mathbf{q}}_{c_r}, \quad (20)$$

with  $\mathbf{u} \triangleq \mathbf{B}_c\boldsymbol{\tau}$ , where  $\mathbf{q}_{c_r} \in \mathcal{C}^2$  stands for the desired reference set to the controlled DOF. Finally, by defining the state vector  $\chi \triangleq [\int_0^\tau \tilde{\mathbf{q}}'_c d\tau \ \tilde{\mathbf{q}}'_c \ \ddot{\tilde{\mathbf{q}}}_c]'$ , system (20) is represented in the standard form

$$\dot{\chi}(t) = \mathbf{f}(\mathbf{q}, \dot{\mathbf{q}}, \ddot{\mathbf{q}}_r, t) + \mathbf{G}(\mathbf{q})\mathbf{u} + \mathbf{K}(\mathbf{q})\mathbf{w}_r, \quad \mathbf{z}_c(t) = \int_0^t \tilde{\mathbf{q}}_c(\tau) d\tau, \quad (21)$$

with  $\mathbf{z}_c(t)$  being the cost variable selected as an integral action over the tracking error  $\tilde{\mathbf{q}}_c$  to provide parametric uncertainty and constant disturbance rejection capability for the CL system, and  $\mathbf{f}(\mathbf{q}, \dot{\mathbf{q}}, \ddot{\mathbf{q}}_r, t) \triangleq [\tilde{\mathbf{q}}'_c \ \ddot{\tilde{\mathbf{q}}}_c \ \mathbf{h}'_c]'$ , with  $\mathbf{h}_c \triangleq M_{cc}^{-1}(-M_{cr}\ddot{\mathbf{q}}_r - C_{cc}\dot{\tilde{\mathbf{q}}}_c - C_{cr}\dot{\mathbf{q}}_r - \mathbf{g}_c) - \ddot{\mathbf{q}}_{c_r}$ , and  $\mathbf{K}(\mathbf{q}) = \mathbf{G}(\mathbf{q}) \triangleq [\mathbf{0} \ \mathbf{0} \ M_{cc}^{-1}]'$ .

Considering (21) and Theorem 1, the nonlinear  $\mathcal{W}_\infty$  control law (10) is obtained, which is given in terms of the generalized input  $\mathbf{u}^* = \mathbf{B}_c \boldsymbol{\tau}$ . From (7),

$$\mathbf{u}^* = \mathbf{B}_c \boldsymbol{\tau} = \mathbf{R}_B^T \mathbf{a}_z f_z = \begin{bmatrix} \cos(\psi) & -\sin(\psi) & 0 \\ \sin(\psi) & \cos(\psi) & 0 \\ 0 & 0 & 1 \end{bmatrix} \begin{bmatrix} \cos(\phi) \sin(\theta) \\ -\sin(\phi) \\ \cos(\phi) \cos(\theta) \end{bmatrix} f_z, \quad (22)$$

where  $\mathbf{B}_c = [\mathbf{R}_B^T \mathbf{a}_z \ \mathbf{R}_B^T \mathbf{a}_z \ \cdots \ \mathbf{R}_B^T \mathbf{a}_z]$ , and  $f_z \triangleq f_{\mathcal{P}_1} + f_{\mathcal{P}_2} + \cdots + f_{\mathcal{P}_8}$  is the total thrust. Therefore, to satisfy (22), we use the following control allocation scheme:

$$f_z = u_3 / (\cos(\phi) \cos(\theta)), \phi_r = \text{asin}(-u_2/f_z), \theta_r = \text{asin}(u_1/(\cos(\phi_r)f_z)), \quad (23)$$

for  $f_z > 0$ ,  $\cos(\phi) \neq 0$ , and  $\cos(\theta) \neq 0$ , where  $\mathbf{u}_i$ , for  $i \in \{1, 2, 3\}$ , stands to the element corresponding to the  $i$ -th row of vector  $\mathbf{u}^*$ , and  $\phi_r$  and  $\theta_r$  stands for the desired references for the roll and pitch angles.

To comply with (23), a second nonlinear  $\mathcal{W}_\infty$  controller is designed taking into account the dynamics of the regulated DOF. Therefore, by replacing  $\ddot{\mathbf{q}}_c$  in the second row of (19), the tracking error dynamics of  $\mathbf{q}_r$  are written as

$$\ddot{\tilde{\mathbf{q}}}_r = -\bar{\mathbf{M}}^{-1}(\bar{\mathbf{C}}\dot{\tilde{\mathbf{q}}}_r + \bar{\mathbf{M}}\ddot{\mathbf{q}}_{r_r} + \bar{\mathbf{C}}\dot{\mathbf{q}}_{r_r} + \bar{\mathbf{e}}) + \bar{\mathbf{B}}\boldsymbol{\tau} + \bar{\boldsymbol{\delta}}, \quad (24)$$

where  $\tilde{\mathbf{q}}_r \triangleq \mathbf{q}_r - \mathbf{q}_{r_r}$ , in which  $\mathbf{q}_{r_r} \in \mathcal{C}^2$  stands for the desired value of the regulated DOF, with  $\phi_r$  and  $\theta_r$  given in (23). Besides,  $\bar{\mathbf{M}}(\mathbf{q}) \triangleq \mathbf{M}_{rr} - \mathbf{M}_{rc}\mathbf{M}_{cc}^{-1}\mathbf{M}_{cr}$ ,  $\bar{\mathbf{C}}(\mathbf{q}, \dot{\mathbf{q}}) \triangleq \mathbf{C}_{rr} - \mathbf{M}_{rc}\mathbf{M}_{cc}^{-1}\mathbf{C}_{cr}$ ,  $\bar{\mathbf{e}}(\mathbf{q}, \dot{\mathbf{q}}) \triangleq \mathbf{g}_r - \mathbf{M}_{rc}\mathbf{M}_{cc}^{-1}\mathbf{g}_c + (\mathbf{C}_{rc} - \mathbf{M}_{rc}\mathbf{M}_{cc}^{-1}\mathbf{C}_{cc})\dot{\mathbf{q}}_c$ ,  $\bar{\mathbf{B}}(\mathbf{q}) = \mathbf{B}_r - \mathbf{M}_{rc}\mathbf{M}_{cc}^{-1}\mathbf{B}_c$ , and  $\bar{\boldsymbol{\delta}}(\mathbf{q}, t) \triangleq \mathbf{w}_r - \mathbf{M}_{rc}\mathbf{M}_{cc}^{-1}\mathbf{w}_c$ .

*Remark 1.* In this work, we set  $\dot{\phi}_r = \dot{\theta}_r = 0$ , for control design purposes based on the time scale separation hypothesis of a cascade control strategy.

Given the state vector  $\mathbf{x} \triangleq [\int_0^t \tilde{\mathbf{q}}_r' d\tau \ \tilde{\mathbf{q}}_r' \ \dot{\tilde{\mathbf{q}}}_r']'$ , (24) is represented as

$$\dot{\mathbf{x}} = \bar{\mathbf{f}}(\mathbf{q}, \dot{\mathbf{q}}, t) + \bar{\mathbf{g}}(\mathbf{q}, t)\bar{\mathbf{u}} + \bar{\mathbf{k}}(\mathbf{q}, t)\bar{\boldsymbol{\delta}}, \quad \mathbf{z}_r = \int_0^t \tilde{\mathbf{q}}_c(\tau) d\tau, \quad (25)$$

with  $\mathbf{z}_r$  being the cost variable, where  $\bar{\mathbf{u}} \triangleq \bar{\mathbf{B}}\boldsymbol{\tau}$ ,  $\bar{\mathbf{d}} \triangleq \bar{\mathbf{M}}\ddot{\mathbf{q}}_{r_r} + \bar{\mathbf{C}}\dot{\mathbf{q}}_{r_r} + \bar{\mathbf{e}}$ , and  $\bar{\mathbf{f}}(\mathbf{q}, \dot{\mathbf{q}}, t) \triangleq [\tilde{\mathbf{q}}_r' \ \dot{\tilde{\mathbf{q}}}_r' \ h_r']'$ ,  $\bar{\mathbf{k}}(\mathbf{q}) = \bar{\mathbf{g}}(\mathbf{q}) \triangleq [\mathbf{0} \ \mathbf{0} \ \bar{\mathbf{M}}^{-1}]'$ . The nonlinear  $\mathcal{W}_\infty$  control law (10) is obtained taking into account (21) and Theorem 1. This OC law is given in terms of the generalized input,  $\bar{\mathbf{u}}^* = \bar{\mathbf{B}}\boldsymbol{\tau}$ . To obtain  $\boldsymbol{\tau}$ , we propose the following control allocation scheme:

$$\min_{\boldsymbol{\tau} \in \mathbb{R}^8} 0.5 (\bar{\mathbf{u}}^* - \bar{\mathbf{B}}\boldsymbol{\tau})' (\bar{\mathbf{u}}^* - \bar{\mathbf{B}}\boldsymbol{\tau}), \quad \text{s.t.} \quad \text{i), ii), and iii),} \quad (26)$$

with i)  $\bar{\mathbf{u}}^* = -\bar{\mathbf{M}}([\mathbf{0} \ \mathbf{0} \ (\mathcal{Y}_3)^{-1}]\mathbf{Q}\mathbf{x} - \bar{\mathbf{M}}^{-1}\bar{\mathbf{C}}\dot{\tilde{\mathbf{q}}}_r - \bar{\mathbf{M}}^{-1}\bar{\mathbf{d}})$ , ii)  $f_{\mathcal{P}_i} - f_{\mathcal{P}_{i+1}} = 0$  and iii)  $\sum_{i=1}^8 f_{\mathcal{P}_i} = f_z$ ,  $\forall i \in \{1, 3, 5, 7\}$ .

*Remark 2.* The minimum  $\bar{\mathbf{u}}^* = \bar{\mathbf{B}}\boldsymbol{\tau}$  to (26) constitutes a set of equations that can be satisfied even with the imposition of constraints ii) and iii) (i.e. five constraints), since  $\boldsymbol{\tau} \in \mathbb{R}^8$  and  $\bar{\mathbf{u}}^* \in \mathbb{R}^3$ .

## 4 Joint state, input and parameter estimation

Consider the nonlinear discrete-time system

$$\begin{aligned} \mathbf{x}_k &= \boldsymbol{\varphi}(\mathbf{x}_{k-1}, \mathbf{u}_{k-1}, \mathbf{d}_{k-1}, \mathbf{p}_{k-1}) + \mathbf{B}_w \mathbf{w}_{k-1}, \\ \mathbf{y}_k &= \boldsymbol{\pi}(\mathbf{x}_k, \mathbf{u}_k, \mathbf{d}_k, \mathbf{p}_k) + \mathbf{D}_v \mathbf{v}_k, \end{aligned} \quad (27)$$

where  $\mathbf{x}_k \in \mathbb{R}^n$  is the system state,  $\mathbf{u}_k \in \mathbb{R}^{n_u}$  is the known input,  $\mathbf{w}_k \in \mathbb{R}^{n_w}$  is the process disturbance,  $\mathbf{y}_k \in \mathbb{R}^{n_y}$  is the measured output,  $\mathbf{v}_k \in \mathbb{R}^{n_v}$  is the measurement disturbance,  $\mathbf{d}_k \in \mathbb{R}^{n_d}$  are unknown exogenous inputs, and  $\mathbf{p}_k \in \mathbb{R}^{n_p}$  are the unknown parameters. In addition,  $\boldsymbol{\varphi} : \mathbb{R}^n \times \mathbb{R}^{n_u} \times \mathbb{R}^{n_d} \times \mathbb{R}^{n_p} \rightarrow \mathbb{R}^n$  and  $\boldsymbol{\pi} : \mathbb{R}^n \times \mathbb{R}^{n_u} \times \mathbb{R}^{n_d} \times \mathbb{R}^{n_p} \rightarrow \mathbb{R}^{n_y}$  are nonlinear mappings. The initial state, exogenous input, model parameters, and disturbances are assumed to satisfy  $\mathbf{x}_0 \sim \mathcal{N}(\hat{\mathbf{x}}_0, \mathbf{P}_0^x)$ ,  $\mathbf{d}_0 \sim \mathcal{N}(\hat{\mathbf{d}}_0, \mathbf{P}_0^d)$ ,  $\mathbf{d}_k - \mathbf{d}_{k-1} \triangleq \Delta \mathbf{d}_{k-1} \sim \mathcal{N}(\mathbf{0}, \mathbf{P}^{\Delta d})$ ,  $\mathbf{p}_0 \sim \mathcal{N}(\hat{\mathbf{p}}_0, \mathbf{P}_0^p)$ ,  $\mathbf{p}_k - \mathbf{p}_{k-1} \triangleq \Delta \mathbf{p}_{k-1} \sim \mathcal{N}(\mathbf{0}, \mathbf{P}^{\Delta p})$ ,  $\mathbf{w}_k \sim \mathcal{N}(\mathbf{0}, \mathbf{P}^w)$ , and  $\mathbf{v}_k \sim \mathcal{N}(\mathbf{0}, \mathbf{P}^v)$ . In order to estimate the exogenous input  $\mathbf{d}_k$  and the unknown parameters  $\mathbf{p}_k$ , we consider the augmented state vector  $\boldsymbol{\mu}_k \triangleq (\mathbf{x}_k, \mathbf{d}_k, \mathbf{p}_k) \in \mathbb{R}^{n_\mu}$ , with  $n_\mu \triangleq n + n_d + n_p$ ,  $\boldsymbol{\mu}_k \sim \mathcal{N}(\hat{\boldsymbol{\mu}}_0, \mathbf{P}_0^\mu)$ , where  $\hat{\boldsymbol{\mu}}_0 \triangleq (\hat{\mathbf{x}}_0, \hat{\mathbf{d}}_0, \hat{\mathbf{p}}_0)$ , and  $\mathbf{P}_0^\mu \triangleq \text{blkdiag}(\mathbf{P}_0^x, \mathbf{P}_0^d, \mathbf{P}_0^p)$ . The system (27) is then rewritten in terms of the augmented variable  $\boldsymbol{\mu}_k$  as

$$\boldsymbol{\mu}_k = \tilde{\boldsymbol{\varphi}}(\boldsymbol{\mu}_{k-1}, \mathbf{u}_{k-1}) + \tilde{\mathbf{B}}_w \tilde{\mathbf{w}}_{k-1}, \quad \mathbf{y}_k = \tilde{\boldsymbol{\pi}}(\boldsymbol{\mu}_k, \mathbf{u}_k) + \mathbf{D}_v \mathbf{v}_k \quad (28)$$

where  $\tilde{\boldsymbol{\varphi}} : \mathbb{R}^{n_\mu} \times \mathbb{R}^{n_u} \rightarrow \mathbb{R}^{n_\mu}$ ,  $\tilde{\boldsymbol{\pi}} : \mathbb{R}^{n_\mu} \times \mathbb{R}^{n_u} \rightarrow \mathbb{R}^{n_y}$ ,  $\tilde{\mathbf{B}}_w \in \mathbb{R}^{n_\mu \times n_w + n_d + n_p}$  and  $\tilde{\mathbf{w}}_{k-1} \in \mathbb{R}^{n_w + n_d + n_p}$  are given by  $\tilde{\boldsymbol{\varphi}}(\boldsymbol{\mu}_{k-1}, \mathbf{u}_{k-1}) \triangleq (\boldsymbol{\varphi}(\mathbf{x}_{k-1}, \mathbf{u}_{k-1}, \mathbf{d}_{k-1}, \mathbf{p}_{k-1}), \mathbf{d}_{k-1}, \mathbf{p}_{k-1})$ ,  $\tilde{\boldsymbol{\pi}}(\boldsymbol{\mu}_k, \mathbf{u}_k) \triangleq \boldsymbol{\pi}(\mathbf{x}_k, \mathbf{u}_k, \mathbf{d}_k, \mathbf{p}_k)$ ,  $\tilde{\mathbf{B}}_w \triangleq \text{blkdiag}(\mathbf{B}_w, \mathbf{I}_{n_d}, \mathbf{I}_{n_p})$ , and  $\tilde{\mathbf{w}}_{k-1} \triangleq (\mathbf{w}_{k-1}, \Delta \mathbf{d}_{k-1}, \Delta \mathbf{p}_{k-1})$ .

Given the augmented system (28),  $\boldsymbol{\mu}_0 \sim \mathcal{N}(\hat{\boldsymbol{\mu}}_0, \mathbf{P}_0^\mu)$ ,  $\tilde{\mathbf{w}}_{k-1} \sim \mathcal{N}(\mathbf{0}, \mathbf{P}^{\tilde{w}})$ ,  $\mathbf{v}_k \sim \mathcal{N}(\mathbf{0}, \mathbf{P}^v)$ , with  $\mathbf{P}^{\tilde{w}} \triangleq \text{blkdiag}(\mathbf{P}^w, \mathbf{P}^{\Delta d}, \mathbf{P}^{\Delta p})$ , the objective is to estimate the tuple  $(\hat{\boldsymbol{\mu}}_k, \hat{\mathbf{P}}_k^\mu)$  for known input and measurement sequences  $(\mathbf{u}_0, \mathbf{u}_1, \dots, \mathbf{u}_{k-1})$  and  $(\mathbf{y}_1, \mathbf{y}_2, \dots, \mathbf{y}_k)$ , respectively. This is done recursively through the joint state, input, and parameter unscented Kalman filter (JUKF) composed of the prediction and update steps described in the following paragraphs.

Let  $\boldsymbol{\mu}_{k-1} \sim \mathcal{N}(\hat{\boldsymbol{\mu}}_{k-1}, \hat{\mathbf{P}}_{k-1}^\mu)$ , and consider the *sigma-point transformation* [6]  $[\hat{\boldsymbol{\mu}}_{k-1}^{(1)} \quad \hat{\boldsymbol{\mu}}_{k-1}^{(2)} \quad \dots \quad \hat{\boldsymbol{\mu}}_{k-1}^{(2n)}] \triangleq \hat{\boldsymbol{\mu}}_{k-1} \mathbf{1}_{1 \times 2n} + \sqrt{n} [\hat{\mathbf{S}}_{k-1}^\mu \quad -\hat{\mathbf{S}}_{k-1}^\mu]$ , where  $\hat{\boldsymbol{\mu}}_{k-1}^{(i)}$  is the  $i$ -th sigma point associated to  $\mathcal{N}(\hat{\boldsymbol{\mu}}_{k-1}, \hat{\mathbf{P}}_{k-1}^\mu)$ , and  $\hat{\mathbf{S}}_{k-1}^\mu$  is the lower triangular matrix obtained from the Cholesky decomposition  $\hat{\mathbf{S}}_{k-1}^\mu (\hat{\mathbf{S}}_{k-1}^\mu)^T = \hat{\mathbf{P}}_{k-1}^\mu$ . Let  $\hat{\boldsymbol{\mu}}_{k-1}^{(i)+} \triangleq \tilde{\boldsymbol{\varphi}}(\hat{\boldsymbol{\mu}}_{k-1}^{(i)}, \mathbf{u}_{k-1})$ , and  $\rho \triangleq 1/(2n)$ , then the predicted tuple  $(\bar{\boldsymbol{\mu}}_k, \bar{\mathbf{P}}_k^\mu)$  is obtained by the *prediction step*  $\bar{\boldsymbol{\mu}}_k = \rho \sum_{i=1}^{2n} \hat{\boldsymbol{\mu}}_{k-1}^{(i)+}$ ,  $\bar{\mathbf{P}}_k^\mu = \tilde{\mathbf{B}}_w \mathbf{P}^{\tilde{w}} \tilde{\mathbf{B}}_w^T + \rho \sum_{i=1}^{2n} (\hat{\boldsymbol{\mu}}_{k-1}^{(i)+} - \bar{\boldsymbol{\mu}}_k)(\hat{\boldsymbol{\mu}}_{k-1}^{(i)+} - \bar{\boldsymbol{\mu}}_k)^T$ . Moreover, consider the sigma-point transformation  $[\bar{\boldsymbol{\mu}}_k^{(1)} \quad \bar{\boldsymbol{\mu}}_k^{(2)} \quad \dots \quad \bar{\boldsymbol{\mu}}_k^{(2n)}] \triangleq \bar{\boldsymbol{\mu}}_k \mathbf{1}_{1 \times 2n} + \sqrt{n} [\bar{\mathbf{S}}_k^\mu \quad -\bar{\mathbf{S}}_k^\mu]$ , where  $\bar{\mathbf{S}}_k^\mu$  is the lower triangular matrix obtained from the Cholesky decomposition  $\bar{\mathbf{S}}_k^\mu (\bar{\mathbf{S}}_k^\mu)^T = \bar{\mathbf{P}}_k^\mu$ . Define  $\bar{\mathbf{y}}_k^{(i)+} \triangleq \tilde{\boldsymbol{\pi}}(\bar{\boldsymbol{\mu}}_k^{(i)}, \mathbf{u}_k)$ , then the predicted tuple  $(\bar{\mathbf{y}}_k, \bar{\mathbf{P}}_k^y, \bar{\mathbf{P}}_k^{\mu y})$  is obtained by  $\bar{\mathbf{y}}_k = \rho \sum_{i=1}^{2n} \bar{\mathbf{y}}_k^{(i)+}$ ,  $\bar{\mathbf{P}}_k^y = \mathbf{D}_v \mathbf{P}^v (\mathbf{D}_v)^T + \rho \sum_{i=1}^{2n} (\bar{\mathbf{y}}_k^{(i)+} - \bar{\mathbf{y}}_k)(\bar{\mathbf{y}}_k^{(i)+} - \bar{\mathbf{y}}_k)^T$ ,  $\bar{\mathbf{P}}_k^{\mu y} = \rho \sum_{i=1}^{2n} (\bar{\boldsymbol{\mu}}_k^{(i)} - \bar{\boldsymbol{\mu}}_k)(\bar{\mathbf{y}}_k^{(i)+} - \bar{\mathbf{y}}_k)^T$ .

Finally, consider the tuple  $(\bar{\boldsymbol{\mu}}_k, \bar{\mathbf{P}}_k^\mu, \bar{\mathbf{y}}_k, \bar{\mathbf{P}}_k^y, \bar{\mathbf{P}}_k^{\mu y})$  obtained in the prediction step. The Kalman gain  $\mathbf{K} \in \mathbb{R}^{n_\mu \times n_y}$  is computed by  $\mathbf{K}_k = \bar{\mathbf{P}}_k^{\mu y} (\bar{\mathbf{P}}_k^y)^{-1}$ , with the estimated tuple  $(\hat{\boldsymbol{\mu}}_k, \hat{\mathbf{P}}_k^\mu)$  being obtained by the *update step*  $\hat{\boldsymbol{\mu}}_k = \bar{\boldsymbol{\mu}}_k + \mathbf{K}_k (\mathbf{y}_k - \bar{\mathbf{y}}_k)$ ,  $\hat{\mathbf{P}}_k^\mu = \bar{\mathbf{P}}_k^\mu - \mathbf{K}_k \bar{\mathbf{P}}_k^y \mathbf{K}_k^T$ .



#### 4.1 Load parameterization, sensors, and control structure

For the sake of simplicity, we consider that the load has a cubic shape with edge length  $2r_L$ , and it is assumed to have homogeneous mass distribution. By defining  $\mathbf{p}_k \triangleq (m_{C_L}, r_L) \in \mathbb{R}^2$ , the inertia tensor  $\mathbb{I}_{C_L}$  and the displacement vector  $\mathbf{d}_{\mathcal{B}, C_L}^{\mathcal{B}}$  are then parameterized as  $\mathbb{I}_{C_L}(\mathbf{p}_k) \triangleq (m_{C_L}/6)r_L^2 \mathbf{I}_3$ , and  $\mathbf{d}_{\mathcal{B}, C_L}^{\mathcal{B}}(\mathbf{p}_k) \triangleq (0, 0, \varsigma(\delta_L + r_L))$ , respectively, where  $\varsigma = -1$  if the load is attached below the UAV,  $\varsigma = 1$  if it is attached above the UAV, and  $\delta_L$  is a known displacement from the origin of  $\mathcal{B}$  to the point of attachment of the load.

Consider (3), with  $\boldsymbol{\vartheta}(\mathbf{q}(t), \boldsymbol{\tau}(t)) = \mathbf{B}(\mathbf{q}(t))\boldsymbol{\tau}(t)$  as in (7). Let  $\mathbf{x}(t) \triangleq (\mathbf{q}(t), \dot{\mathbf{q}}(t)) \in \mathbb{R}^{12}$  and  $\mathbf{u}(t) \triangleq \boldsymbol{\tau}(t) \in \mathbb{R}^8$ , and using the forward Euler discretization method (FEDM) with sampling time  $T_s$ , we have that  $\mathbf{x}_k = \mathbf{x}_{k-1} + T_s \dot{\mathbf{x}}(t)|_{t=(k-1)T_s} + \boldsymbol{\ell}_{k-1}$ , where  $\boldsymbol{\ell}_{k-1} \in \mathbb{R}^{12}$  is the discretization error. Moreover, for state estimation, we consider that  $\boldsymbol{\zeta}_k \triangleq [\mathbf{I}_2 \mathbf{0}_{2 \times 4}]' \mathbf{d}_k + \boldsymbol{\varpi}_k$ , with  $\mathbf{d}_k \in \mathbb{R}^2$  being exogenous inputs, and  $\boldsymbol{\varpi}_k \in \mathbb{R}^6$  being modeling uncertainties. In addition, we define the vector of process disturbances as  $\mathbf{w}_{k-1} \triangleq \begin{bmatrix} \mathbf{0}_{6 \times 6} \\ (\mathbf{M}(\mathbf{x}_{k-1}, \mathbf{p}_{k-1}))^{-1} \end{bmatrix} \boldsymbol{\varpi}_{k-1} + \boldsymbol{\ell}_{k-1}$ . Hence, the state-space equations for joint estimation of the OUAV are given in discrete time by  $\mathbf{x}_k = \boldsymbol{\varphi}(\mathbf{x}_{k-1}, \mathbf{u}_{k-1}, \mathbf{d}_{k-1}, \mathbf{p}_{k-1}) + \mathbf{w}_{k-1}$ , where

$$\boldsymbol{\varphi}(\mathbf{x}_{k-1}, \mathbf{u}_{k-1}, \mathbf{d}_{k-1}, \mathbf{p}_{k-1}) \triangleq \mathbf{x}_{k-1} + T_s \begin{bmatrix} [\mathbf{0} \ \mathbf{I}_6] \mathbf{x}_{k-1} \\ \boldsymbol{\iota}(\mathbf{x}_{k-1}, \mathbf{u}_{k-1}, \mathbf{d}_{k-1}, \mathbf{p}_{k-1}) \end{bmatrix}, \quad (29)$$

and  $\boldsymbol{\iota}(\mathbf{x}_{k-1}, \mathbf{u}_{k-1}, \mathbf{d}_{k-1}, \mathbf{p}_{k-1}) \triangleq (\mathbf{M}(\mathbf{x}_{k-1}, \mathbf{p}_{k-1}))^{-1} (-\mathbf{C}(\mathbf{x}_{k-1}, \mathbf{p}_{k-1})[\mathbf{0} \ \mathbf{I}_6] \mathbf{x}_{k-1} - \mathbf{g}(\mathbf{x}_{k-1}, \mathbf{p}_{k-1}) + \mathbf{B}(\mathbf{x}_{k-1}) \mathbf{u}_{k-1} + [\mathbf{I}_2 \ \mathbf{0}_{2 \times 4}]' \mathbf{d}_{k-1})$ .

For design of the JUKF, we consider that a Global Positioning System (GPS), a barometer, an accelerometer, a gyroscope and a magnetometer are available onboard the OUAV. The following variables are assumed to be measured: the position of the UAV w.r.t to the inertial frame  $\mathcal{I}$ ,  $\boldsymbol{\xi}_k = [x_k \ y_k \ z_k]^T$ , the orientation of the UAV w.r.t.  $\mathcal{I}$ ,  $\boldsymbol{\eta}_k = [\phi_k \ \theta_k \ \psi_k]^T$ , and the angular velocity  $\mathbf{w}_{\mathcal{I}, \mathcal{B}}^{\mathcal{B}}$ . The measurement  $\mathbf{y}_k \in \mathbb{R}^9$  is described by the measurement equation  $\mathbf{y}_k = \boldsymbol{\pi}(\mathbf{x}_k, \mathbf{u}_k, \mathbf{d}_k, \mathbf{p}_k) + \mathbf{v}_k$ , with  $\boldsymbol{\pi}(\mathbf{x}_k, \mathbf{u}_k, \mathbf{d}_k, \mathbf{p}_k) \triangleq (\boldsymbol{\xi}_k, \boldsymbol{\eta}_k, \mathbf{w}_{\mathcal{I}, \mathcal{B}}^{\mathcal{B}}) = (\boldsymbol{\xi}_k, \boldsymbol{\eta}_k, \mathbf{W}_{\boldsymbol{\eta}}(\boldsymbol{\eta}_k) \dot{\boldsymbol{\eta}}_k)$ , where  $\mathbf{W}_{\boldsymbol{\eta}}(\boldsymbol{\eta}_k)$  defined as in Section 2. Finally, let  $\boldsymbol{\mu}_k \triangleq (\mathbf{x}_k, \mathbf{d}_k, \mathbf{p}_k) \in \mathbb{R}^{16}$ , with  $\boldsymbol{\mu}_k \sim \mathcal{N}(\hat{\boldsymbol{\mu}}_0, \mathbf{P}_0^{\mu})$ , where  $\hat{\boldsymbol{\mu}}_0 \triangleq (\hat{x}_0, \hat{d}_0, \hat{p}_0)$ , and  $\mathbf{P}_0 \triangleq \text{blkdiag}(\mathbf{P}_0^x, \mathbf{P}_0^d, \mathbf{P}_0^p)$ . Then,  $\tilde{\boldsymbol{\varphi}}$ ,  $\tilde{\boldsymbol{\pi}}$ ,  $\tilde{\mathbf{B}}_w$ ,  $\mathbf{D}_v$  in (28) are  $\tilde{\boldsymbol{\varphi}}(\boldsymbol{\mu}_{k-1}, \mathbf{u}_{k-1}) \triangleq (\boldsymbol{\varphi}(\mathbf{x}_{k-1}, \mathbf{u}_{k-1}, \mathbf{d}_{k-1}, \mathbf{p}_{k-1}), \mathbf{d}_{k-1}, \mathbf{p}_{k-1})$ ,  $\tilde{\boldsymbol{\pi}}(\boldsymbol{\mu}_k, \mathbf{u}_k) \triangleq (\boldsymbol{\xi}_k, \boldsymbol{\eta}_k, \mathbf{W}_{\boldsymbol{\eta}}(\boldsymbol{\eta}_k) \dot{\boldsymbol{\eta}}_k)$ ,  $\tilde{\mathbf{B}}_w = \mathbf{I}_{16}$ ,  $\mathbf{D}_v = \mathbf{I}_9$ , with  $\boldsymbol{\varphi}(\mathbf{x}_{k-1}, \mathbf{u}_{k-1}, \mathbf{d}_{k-1}, \mathbf{p}_{k-1})$  defined as in (29). Hence, the JUKF for the OUAV with load is composed by the prediction and update steps described previously in this section. Using the known input  $\mathbf{u}_k$  and the measurement vector  $\mathbf{y}_k$ , the JUKF provides estimates of the states and load parameters to the nonlinear  $\mathcal{W}_{\infty}$  controller.

## 5 Numerical experiments

This section conducts a numerical experiment, using MATLAB R2017a, to corroborate the efficacy of the proposed control strategy. The differential equations composing the control system were discretized using the FEDM with sampling time  $T_s = 0.01$  s, and the OUAV physical parameters are given in

Table 1 (drag and thrust constants estimated based on the brushless TMotor U15II KV100 with propeller G40x13.1CF, <https://store.tmotor.com/goods.php?id=732>). Moreover, for simulation purposes,  $m_{c_L} = 100$  kg and  $r_L = 0.5$  m.

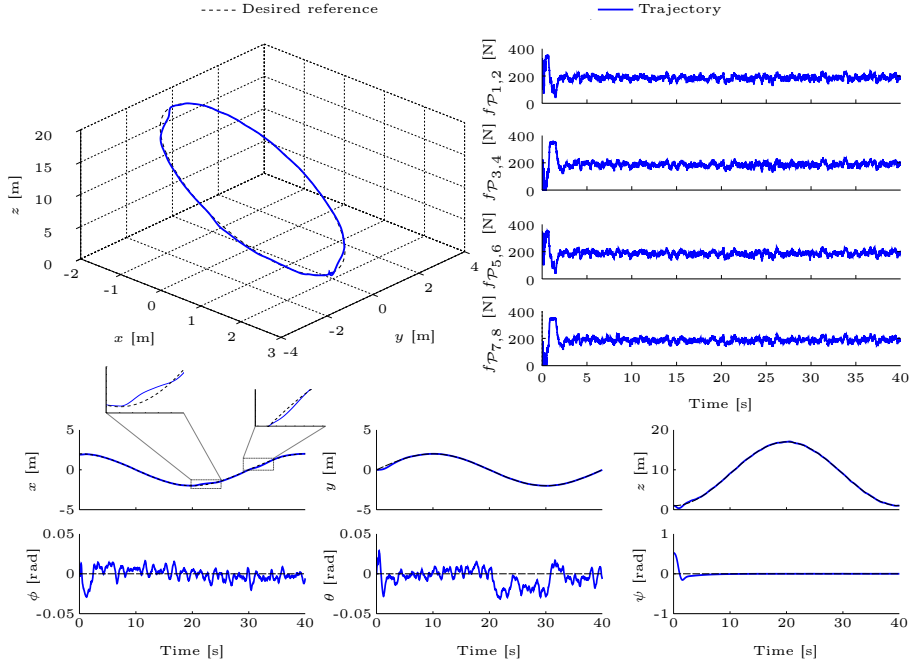
To implement the nonlinear  $\mathcal{W}_\infty$  controller proposed in Section 3, the OC law,  $\mathbf{u}^*$ , for the controlled DOF dynamics (21), was tuned via Brynson's method. Then, a fine tuning was performed over the initial tuning, which resulted in  $\mathbf{Y}_0^{(c)} = \text{diag}(5, 5, 10)$ ,  $\mathbf{Y}_1^{(c)} = \text{diag}(10, 10, 50)$ ,  $\mathbf{Y}_2^{(c)} = \text{diag}(1, 1, 1)$ ,  $\mathbf{Y}_3^{(c)} = \text{diag}(6, 6, 1)$ . The same tuning process was considered to the OC law,  $\mathbf{u}^*$ , for the regulated DOF dynamics (25), which resulted in  $\mathbf{Y}_0^{(r)} = \text{diag}(1, 1, 1)$ ,  $\mathbf{Y}_1^{(r)} = \text{diag}(10, 10, 10)$ ,  $\mathbf{Y}_2^{(r)} = \text{diag}(0.2, 0.2, 0.2)$ ,  $\mathbf{Y}_3^{(r)} = \text{diag}(0.05, 0.05, 0.05)$ . To execute the nonlinear  $\mathcal{W}_\infty$  controller, first, the desired values to the roll,  $\phi_r$ , and pitch,  $\theta_r$ , angles, and the total thrust  $f_z$  are computed from (23). Then, the OC allocation scheme (26) is solved to obtain  $\boldsymbol{\tau}$ , which is applied to (3). The nonlinear  $\mathcal{W}_\infty$  controller is computed using  $(\hat{\mathbf{x}}_k, \hat{\mathbf{p}}_k)$  estimated by the JUKF proposed in Section 4. The controller is executed at each sampling time  $T_s$ , while the discrete-time design of the JUKF takes advantage of the sampling nature of the measurement  $\mathbf{y}_k$ . The JUKF was designed with  $\mathbf{P}^{\bar{w}} = \text{diag}((\frac{0.01}{3})^2 \cdot \mathbf{1}_{12 \times 1}, (\frac{1}{3})^2 \cdot \mathbf{1}_{2 \times 1}, (\frac{2}{3})^2, (\frac{0.001}{3})^2)$ ,  $\mathbf{P}^v = \text{diag}(0.05^2 \cdot \mathbf{1}_{2 \times 1}, 0.17^2, (\frac{0.05\pi}{180})^2 \cdot \mathbf{1}_{3 \times 1}, 0.00552^2 \cdot \mathbf{1}_{3 \times 1})$ ,  $\mathbf{P}_0^x = \text{diag}((\frac{2}{3})^2 \cdot \mathbf{1}_{3 \times 1}, (\frac{\pi}{18})^2 \cdot \mathbf{1}_{2 \times 1}, (\frac{\pi}{6})^2, (\frac{1}{3})^2 \cdot \mathbf{1}_{3 \times 1}, (\frac{\pi}{36})^2 \cdot \mathbf{1}_{3 \times 1})$ ,  $\mathbf{P}_0^d = \text{diag}((\frac{1}{3})^2 \cdot \mathbf{1}_{2 \times 1})$ ,  $\mathbf{P}_0^p = \text{diag}((\frac{50}{3})^2, (\frac{0.75}{3})^2)$ ,  $\bar{\mathbf{x}}_0 = (2.4, 0.5, -0.2, \frac{\pi}{6}, \frac{\pi}{6}, 0, \mathbf{0}_{6 \times 1})$ ,  $\bar{\mathbf{d}}_0 = (0, 0)$ , and  $\bar{\mathbf{p}}_0 = (50, 0.75)$ . The OUAV was prompted to perform the desired trajectory  $x_r(t) = 2 \cos(2\pi t/40)$  m,  $y_r(t) = 2 \sin(2\pi t/40)$  m,  $z_r(t) = 9 - 8 \cos(2\pi t/40)$  m, and  $\psi_r(t) = 0$  rad, starting displaced from the desired trajectory with the initial conditions  $\mathbf{q}(0) = [1.9 \ 0 \ 0.8 \ 0 \ 0 \ \pi/6]'$  and  $\dot{\mathbf{q}}(0) = \mathbf{0}$ . The disturbance  $\zeta_x(t) = 30$  N, for  $20 \leq t \leq 30$ , is applied to the system. Figure 2 presents the results obtained by the control strategy, and Figure 3 illustrates the time evolution of the states, exogenous disturbances, and load parameters estimated by the JUKF. It can be noticed that the JUKF was able to estimate the generalized DOF,  $\mathbf{q}$ , the generalized velocities,  $\dot{\mathbf{q}}$ , the disturbances,  $\zeta_x$  and  $\zeta_y$ , and the load parameters,  $m_{c_L}$  and  $r_L$ , and provided these information to the nonlinear  $\mathcal{W}_\infty$  controller. The proposed robust control scheme based on the multi-body approach was capable of performing the heavy load transportation subjected to load parameter uncertainties, while maintaining the system stable and attenuating the effects of the exogenous disturbances.

## 6 Conclusions

This work proposed a joint state-parameter observer-based controller for trajectory tracking of an OUAV, for transportation of a heavy load with unknown mass and size. A multi-body dynamic model of the OUAV with a rigidly attached load was obtained, effectively considering the effects of the load parameters. A nonlinear  $\mathcal{W}_\infty$  controller was designed for optimal trajectory tracking of the OUAV, with states and load parameters provided by a UKF-based algorithm. The effectiveness of our approach was corroborated by numerical results, which was capable of performing the load transportation subjected to parameter uncertainties and exogenous disturbances. Future work will consider a wind disturbance model, the load connected through a rope, and perform real flight experiments.

**Table 1.** Octocopter UAV physical parameters.

Parameter	Value	Parameter	Value
$\mathbb{I}_{C_O}$	diag(18.78, 19.76, 37.87) kg.m <sup>2</sup>	$\alpha_1, \alpha_2$	$\pi/4$ (45) rad (deg)
$m_{C_O}$	53.09 kg	$\alpha_3, \alpha_4$	$3\pi/4$ (135) rad (deg)
$g$	-9.81 m/s <sup>2</sup>	$\alpha_5, \alpha_6$	$5\pi/4$ (225) rad (deg)
$\lambda_{P_1}, \lambda_{P_3}, \lambda_{P_5}, \lambda_{P_7}$	1	$\alpha_7, \alpha_8$	$7\pi/4$ (315) rad (deg)
$\lambda_{P_2}, \lambda_{P_4}, \lambda_{P_6}, \lambda_{P_8}$	-1	$b$	$2.85 \cdot 10^{-5}$ N.s <sup>2</sup>
$d_{B,C_O}^B$	(0, 0, 0) m	$k_\tau$	$1.42 \cdot 10^{-6}$ N.m.s <sup>2</sup>
$d_{B,P_1}^B$	(1.1, 1.1, 0.12) m	$d_{B,P_5}^B$	(-1.1, -1.1, 0.12) m
$d_{B,P_2}^B$	(1.1, 1.1, -0.17) m	$d_{B,P_6}^B$	(-1.1, -1.1, -0.17) m
$d_{B,P_3}^B$	(-1.1, 1.1, 0.12) m	$d_{B,P_7}^B$	(1.1, -1.1, 0.12) m
$d_{B,P_4}^B$	(-1.1, 1.1, -0.17) m	$d_{B,P_8}^B$	(1.1, -1.1, -0.17) m
$m_{C_L}$	$\in [0, 100]$ kg	$\mathbb{I}_{C_L}$	$(m_{C_L}/6)r_L^2 \cdot \mathbf{I}_3$ kg.m <sup>2</sup>
$r_L$	$\in [0, 1.5]$ m	$d_{B,C_L}^B$	(0, 0, $-\varsigma(\delta_L + r_L)$ ) m

**Figure 2.** The OUAV trajectory, and the time evolution of  $\mathbf{u}(t)$  and  $\mathbf{q}(t)$ .

## Bibliography

- [1] M. Bernard, K. Kondak, I. Maza, and A. Ollero. Autonomous transportation and deployment with aerial robots for search and rescue missions. *Journal of Field Robotics*, 28(6):914–931, October 2011.
- [2] M. Bisgaard. *Modeling, Estimation and Control of Helicopter Slung Load System*. PhD thesis, Aalborg University, 2008.

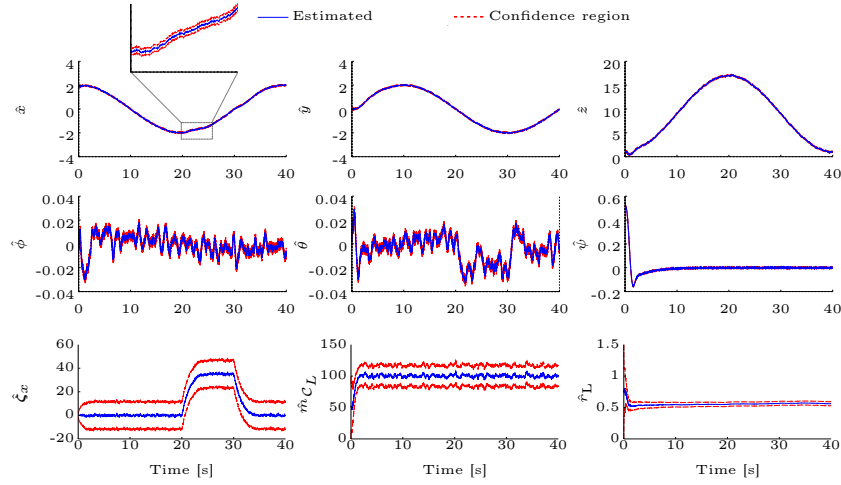


**Figure 3.** Estimated generalized DOF, disturbances and load parameters.

- [3] M. Bisgaard, A. I. Cour-Harbo, and J. D. Bendtsen. Adaptive control system for autonomous helicopter slung load operations. *Control Engineering Practice*, 18(7):800–811, July 2010.
- [4] D. N. Cardoso, S. R. Esteban, and G. V. Raffo. A robust optimal control approach in the weighted sobolev space for underactuated mechanical systems. *Automatica*, 125:1–11, 2021.
- [5] S. Gajbhiye, D. Cabecinhas, C. Silvestre, and R. Cunha. Geometric finite-time inner-outer loop trajectory tracking control strategy for quadrotor slung-load transportation. *Nonlinear Dynamics*, 107(3):2291–2308, 2022.
- [6] S. Juiler, J. Uhlmann, and H. F. Durrant-Whyte. A new method for the nonlinear transformations of means and covariances in filters and estimations. *IEEE Trans. on Automatic Control*, 45(3):477–482, 2000.
- [7] I. Palunko, A. Faust, P. Cruz, L. Tapia, and R. Fierro. A reinforcement learning approach towards autonomous suspended load manipulation using aerial robots. In *Proc. of the IEEE ICRA*, pages 4881–4886, May 2013.
- [8] V. Prkačin, I. Palunko, and I. Petrović. State and parameter estimation of suspended load using quadrotor onboard sensors. In *Proc. of the IEEE 2020 ICUAS*, pages 958–967, 2020.
- [9] M. W. Spong, S. Hutchinson, M. Vidyasagar, et al. *Robot modeling and control*, volume 3. Wiley New York, 2006.
- [10] K. Sreenath, T. Lee, and V. Kumar. Geometric control and differential flatness of a quadrotor UAV with a cable-suspended load. In *Proc. of the 52nd IEEE CDC*, pages 2269–2274, December 2013.
- [11] F. Wang, P. Liu, S. Zhao, B. M. Chen, S. K. Phang, S. Lai, T. H. Lee, and C. Cai. Guidance, navigation and control of an unmanned helicopter for automatic cargo transportation. In *Proc. of the IEEE 33rd CCC*, pages 1013–1020, July 2014.
- [12] G. Yu, D. Cabecinhas, R. Cunha, and C. Silvestre. Adaptive control with unknown mass estimation for a quadrotor-slung-load system. *ISA Transactions*, 133:412–423, 2023.